classes of photons having equal intensity and their combined effect G_i, showing the resulting 2 maxima required for resolution, are plotted in Fig. 3. Also plotted are the two limiting extremes by which the relative intensity of the γ_3 class may vary and still show one peak conductance per class. As can be seen, the intensity of γ_3 in this example can range from 0.1 to 4 times the equal-intensity case.

CONCLUSIONS

It has been shown that by specifying the thickness of each receiver in an array of photoconductors, the magnitude of the photocurrent through each receiver can be regulated. General equations relating receiver conductance and the absorption coefficient associated with the radiation have been derived, together with equations governing resolution.

The specific case analyzed, in which receiver thicknesses increase by an arithmetic progression, indicates that a maximum current will occur uniquely in one of the inner receivers as a function of the energy of the incident photons. If the photon energies are not too heterogeneous, it is possible to resolve the photons into an energy spectrum.

Though it is beyond the purpose of this paper, it can be pointed out that interesting differences in receiver conductances exist in response to photon influxes when receiver thicknesses are made to vary in manners other than that shown in this paper. Constant thickness receivers exhibit conductances which fall off exponentially at a rate associated with the incident photon energy, thus indicating in one display the fall-off of photon intensity as depth penetrated. If the receivers are arranged so that each shows identical conductance to one class of photons, then other classes indicate their presence by the nonidentical conductances that occur. Interesting response differences to heterogeneous photon mixtures result when thicknesses are made to vary by a prescribed d factor, and an occasional receiver having an odd thickness is inserted between the members of the regular array. In general, it is possible, in this manner to enhance the resolution between two known photon classes, or to make the resulting conductance curves assume required shapes.

JOURNAL OF APPLIED PHYSICS VOLUME 29, NUMBER 1 JANUARY, 1958

Propagation of Waves in Helical Wave Guides*

CHIAO-MIN CHU
Department of Electrical Engineering, The University of Michigan, Ann Arbor, Michigan
(Received May 17, 1957)

The field configuration near the conductors of a helical wave guide is obtained from the solution of the spatial-wave equation for a developed helix. This solution is first obtained for the case of tape conductors and then adapted to elliptical (including circular) conductors by conformal transformation. By comparing this solution with that of a developed-sheath helix, the impedance, attenuation, and other parameters of a wire helix are deduced approximately. These are expressed as the product of the corresponding sheath-helix parameter times a proper correction factor depending on frequency, conductor size, and shape. The analysis is extended to the multifilar helix. The results of this analysis provide a means of calculating the attenuation of wire helices and of choosing optimum wire configurations in the design of helical wave guides.

INTRODUCTION

THE extensive use of helix slow-wave structures in traveling-wave tubes has prompted numerous investigations of the properties of helical guides. However, the only helical configuration for which a rigorous solution has been obtained to date is the sheath-helix model.[1] Helices of thin tapes have been studied by Sensiper,[2] using approximate boundary conditions. Sensiper's results, so far as dispersion characteristics are concerned, agree well with the results of experiment.[3] But his calculations of the attenuation of helical conductors are less defensible. Hosono[4] also attempted to find the attenuation of wire helices, approximating the current as a helical line element. Therefore, his results are valid only for small wires.

In this paper an analysis is presented suitable for determining the effects of wire size and shape on the attenuation and harmonic fields of monofilar and multifilar helices. The analysis is based on the developed helix model,[5] to simplify the mathematical tasks involved. A rigorous solution is presented for developed

* This work was conducted by Project Michigan under Department of the Army Contact DA-36-039 sc-52654, administered by the U. S. Army Signal Corps, operating under a tri-service charter.

[1] J. R. Pierce, *Traveling-Wave Tubes* (D. Van Nostrand Company, Inc., New York, 1950), p. 229.

[2] S. Sensiper, "Electromagnetic wave propagation on helical conductors," Report No. 194, Research Laboratory of Electronics, Massachusetts Institute of Technology, Cambridge, Massachusetts (May, 1954).

[3] D. A. Watkins and A. E. Siegman, J. Appl. Phys. 24, 917 (1953).

[4] T. Hosono, J. Elec. Commun. Eng. Japan 38, 974 (1955).

[5] See reference 1, p. 31.

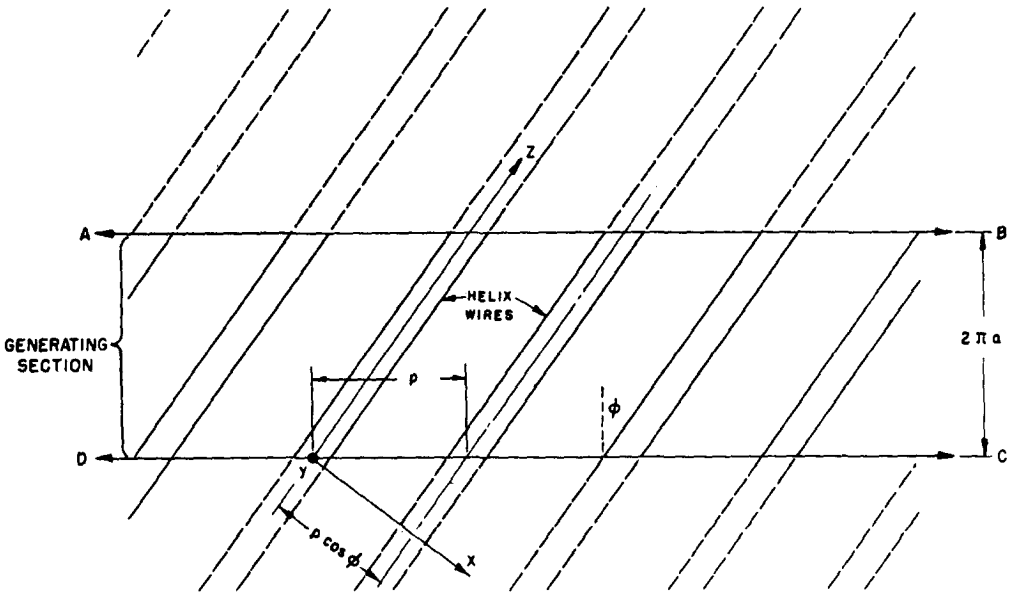

FIG. 1. Developed helix showing the generating section and the periodic extensions.

monofilar and multifilar thin tape conductors. A general procedure is described for extending this solution, by conformal mapping, to obtain a rigorous solution for a wide variety of developed thick conductors. This procedure is specifically applied to find the field configuration when wires of elliptical (including circular) cross section are used. The attenuation, coupling impedance, and other parameters of elliptical-wire helices are then calculated and are described in some detail. The results presented are given with reference to the properties of a true-sheath helix of the same propagation constant.

The errors involved in basing the theory on the developed model arise mainly from: (a) neglecting dispersion, and (b) neglecting the unequal distribution of current on the parts of wire inside and outside of the mean diameter. The net error should be negligible if:

(1) the circumference of the helix is several times the guide wavelength, and
(2) the thickness of the wire is small compared to the radius of the helix.

Subject to these restrictions, the results of the present work should offer a reasonable criterion for the selection of shape and size of conductors, and a means of calculating the power loss with reasonable accuracy.

WAVE EQUATION FOR A DEVELOPED HELIX

The helix to be investigated is assumed to have the following dimensions (monofilar, for the moment):

mean radius: a,
pitch: p, and
pitch angle: $\varphi=\tan^{-1}(p/2\pi a)$.

By cutting an axial slit on the circumference of the helix and flattening the wires into straight conductors, a system of parallel conductors is obtained as shown in section ABCD of Fig. 1. The periodicity of the wave function along the circumference of a helix permits the extension of the conductors to infinity at both ends. Thus, the problem of a helical wave guide is reduced approximately to that of infinite wires supporting a periodic field. With a right-hand coordinate system x, y, z as shown in Fig. 1, the cross section of the conductors in the x-y plane is given by Fig. 2. (For conductors in other than tape form, x' and y' are used.) For convenience, the coordinates are normalized with respect to the period $p\cos\varphi/2\pi$.

At a fixed frequency defined by a propagation constant $\beta_0=\omega/c=2\pi/\gamma$, the field around the infinite system of straight parallel conductors may be generated by the spatial-wave function[6-8]

$$II=II_1(x,y)\exp(-j\beta_0 z). \tag{1}$$

The electric and magnetic fields generated by II are

$$E_z=0,$$

$$E_x=-j\beta_0\frac{2\pi}{p\cos\varphi}\frac{\partial II_1}{\partial x}\exp(-j\beta_0 z),$$

and

$$E_y=-j\beta_0\frac{2\pi}{p\cos\varphi}\frac{\partial II_1}{\partial y}\exp(-j\beta_0 z); \tag{2}$$

and

$$H_z=0,$$

$$H_x=j\omega\epsilon\frac{2\pi}{p\cos\varphi}\frac{\partial II_1}{\partial y}\exp(-j\beta_0 z),$$

$$H_y=-j\omega\epsilon\frac{2\pi}{p\cos\varphi}\frac{\partial II_1}{\partial x}\exp(-j\beta_0 z). \tag{3}$$

[6] Eq. (1) is valid if the conductors are of zero resistivity. It will be assumed conductors of a small finite resistivity support identical first-order fields.

[7] J. A. Stratton, *Electromagnetic Theory* (McGraw-Hill Book Company, Inc., New York, 1941), p. 351.

[8] A. Sommerfield, *Electrodynamics* (Academic Press, Inc., New York, 1952), p. 159.

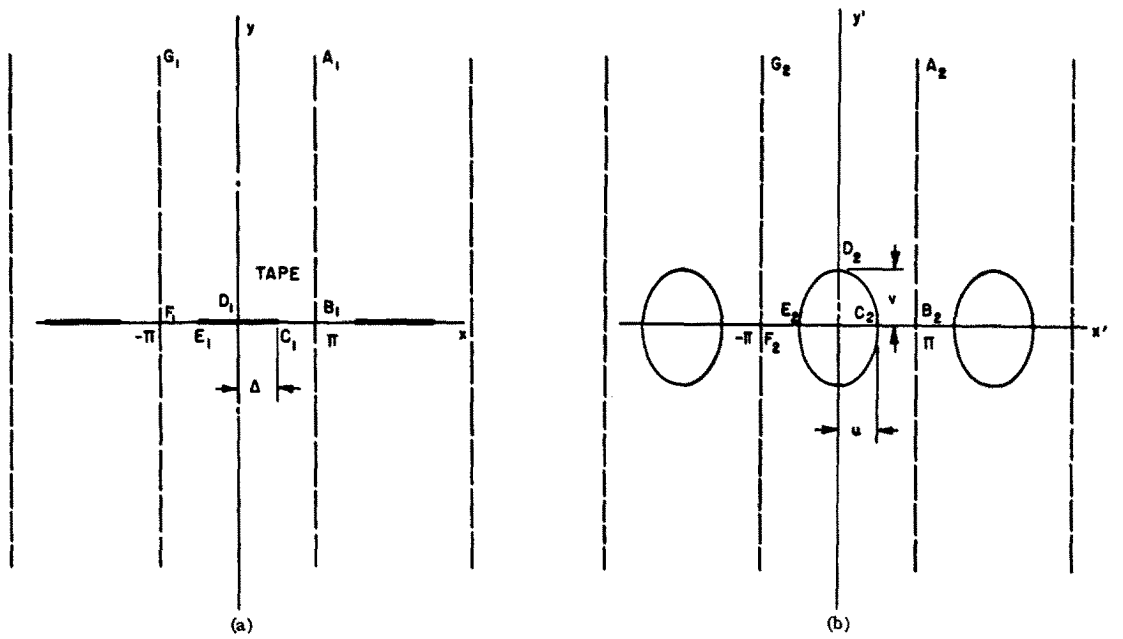

FIG. 2. Cross section perpendicular to the wires of a developed helix showing one unit cell and its periodic extension. (a) Tape of width $\Delta(p\cos\varphi/\pi)$. (b) Elliptic wire of dimension $u(p\cos\varphi/\pi)\cdot v(p\cos\varphi/\pi)$.

The net power flow will be in the direction along the conductors.

Since II satisfies the wave equation, II_1 must satisfy the Laplace equation

$$\frac{\partial^2 II_1}{\partial x^2}+\frac{\partial^2 II_1}{\partial y^2}=0, \tag{4}$$

which permits conformal transformation in the x-y plane.

The solution II_1 in Eq. (4) must also satisfy the periodicity condition inherited from the development from a helix: the phase of the fields around adjacent conductors must differ by a constant amount $2\pi s$ in the x direction. Here s is related to the propagation constant β, or to the number of turns per guided wavelength N, by[9]

$$s=\cos^2\varphi/N, \tag{5a}$$

$$=\beta a\sin\varphi\cos\varphi, \tag{5b}$$

$$=\beta_0 a\cos\varphi. \tag{5c}$$

If $s\neq$integer,[10] any solution of Eq. (4) satisfying the above requirement may be represented as:

$$II_1=\sum_{n=-\infty}^{n=+\infty}\frac{A_n}{|n+s|}\exp[-j(n+s)x\pm|n+s|y], \tag{6}$$

where the positive sign is used for $y<0$, and the negative sign for $y>0$. The A_n's are constants determined by the boundary conditions on the surface of the conductors. For operation of a helix as a slow-wave structure, $0<s<1$, and Eq. (6) may be written as $(y>0)$:

$$II_1=\sum_{n=0}^{\infty}\frac{B_n}{n+s}\exp[-j(n+s)(x-jy)]+\sum_{n=0}^{\infty}\frac{C_n}{n+1-s}\exp[j(n+1-s)(x+jy)]. \tag{7}$$

For $y<0$, $x\pm jy$ should be replaced by their complex conjugates. For $s>1$, s should be replaced by $s-[N_s]$ where $[N_s]$ is the greatest integer less than s.

TAPE HELIX[11]

For a tape helix, the boundary conditions determining B_n and C_n are noted from Fig. 2(a). At $y=0$, E_x must vanish on the tape and E_y must be continuous at the gap. From Eqs. (2) and (7) these conditions can be written as,

$$\sum_{n=0}^{\infty}B_n\exp(-jnx)-\sum_{n=0}^{\infty}C_n\exp[j(n+1)x]=0 \qquad (\Delta>|x|>0), \tag{8a}$$

[9] Equation (5c) is exactly satisfied in a developed helix, but only approximately in a real helix.

[10] The condition $s=$an integer is excluded, since it leads to lateral radiation. In an end-fed true helix, this condition implies that no propagating mode can be supported.

[11] The solution for tape conductors, expressed in integral form, has been obtained independently by P. N. Butcher. See P. N. Butcher, "On the coupling impedance of tape structures," Memo No. 1253, Radar Research Establishment, Malvern, England (1956).

and

$$\sum_{n=0}^{\infty} B_n \exp(-jnx)+\sum_{n=0}^{\infty} C_n \exp[j(n+1)x]=0 \qquad (\pi>|x|>\Delta). \quad (8b)$$

The solution for B_n and C_n from Eq. (8) is not obvious. The usual technique of approximate solution would lead to an attempt at solution of an infinite set of simultaneous equations very difficult to handle. Fortunately, an exact and convenient solution can be obtained by inspection, by use of Legendre polynomials. The following identity is known to exist[12]:

$$\sum_{n=0}^{\infty} P_n(\cos\Delta)\cos(n+\tfrac{1}{2})\theta = \begin{cases} (\cos\theta-\cos\Delta)^{-\frac{1}{2}}/\sqrt{2} & (\Delta>|\theta|>0) \\ 0 & (\pi>|\theta|>\Delta), \end{cases} \quad (9)$$

so

$$\sum_{n=0}^{\infty} P_n(\cos\Delta)\exp(-jn\theta) + \sum_{n=0}^{\infty} P_n(\cos\Delta)\exp[j(n+1)\theta] = \begin{cases} 0 & (\pi>|\theta|>\Delta) \\ \left(\dfrac{2}{\cos\theta-\cos\Delta}\right)^{\frac{1}{2}} \exp\left(j\dfrac{\theta}{2}\right) & (\Delta>|\theta|>0). \end{cases} \quad (10a)$$

Similarly, if, Δ is replaced by $\pi-\Delta$ and θ is replaced by $\pm(\pi-\theta)$ in Eq. (9),

$$\sum_{n=0}^{\infty} P_n(\cos\Delta)\exp(-jn\theta) - \sum_{n=0}^{\infty} P_n(\cos\Delta)\exp[j(n+1)\theta] = \begin{cases} 0 & (\Delta>\theta>0) \\ -j\left(\dfrac{2}{(\cos\Delta-\cos\theta)}\right)^{\frac{1}{2}} \exp\left(j\dfrac{\theta}{2}\right) & (\pi>\theta>\Delta) \\ j\left(\dfrac{2}{(\cos\Delta-\cos\theta)}\right)^{\frac{1}{2}} \exp\left(j\dfrac{\theta}{2}\right) & (-\Delta>\theta>-\pi). \end{cases} \quad (10b)$$

Comparing Eq. (8) with Eq. (10) shows the former satisfied by

$$C_n=B_n=\left(-\frac{E}{\beta_0}\frac{p\cos\varphi}{2\pi}\right)P_n(\cos\Delta), \quad (11)$$

where E is a constant, the amplitude of the "fundamental" electric field. For $y>0$, the exact solution is

$$II=-\frac{E}{\beta_0}\frac{p\cos\varphi}{2\pi}\exp(-j\beta_0 z)\left\{\sum_{n=0}^{\infty}\frac{P_n(\cos\Delta)}{n+s}\times\exp[-j(n+s)(x-jy)]+\sum_{n=0}^{\infty}\frac{P_n(\cos\Delta)}{n+1-s}\times\exp[j(n+1-s)(x+jy)]\right\}. \quad (12)$$

The fields around a tape in the cell $(2q+1)\pi>x>(2q-1)\pi$ differ only by a factor $\exp(-j2\pi s\cdot q)$ from those in $\pi>x>-\pi$, as required. From Eq. (12), the power, circuit voltage, current density, and wire current can be calculated easily.

The power flowing axially along the helix, which equals the power flowing along the strip ABCD in Fig. 1, is expressed by:

$$W=\frac{1}{2\pi}\left(\frac{\epsilon}{\mu}\right)^{\frac{1}{2}}E^2(p\cos\varphi)^2\sum_{n=0}^{\infty}P_n^2(\cos\Delta)\times\left(\frac{1}{n+s}+\frac{1}{n+s-1}\right), \quad (13)$$

or, in closed form,

$$W=\frac{1}{2}\left(\frac{\epsilon}{\mu}\right)^{\frac{1}{2}}E^2(p\cos\varphi)^2\frac{1}{\sin s\pi}P_{-s}(\cos\Delta)P_{-s}(\cos\Delta'), \quad (14)$$

where $\Delta'=\pi-\Delta$.[13,14]

A "circuit voltage," independent of the path of integration, is easily fround from the endpoint values of II_1 or, alternatively, from

$$V_{x=0}=\frac{p\cos\varphi}{2\pi}\int_0^{\infty}E_y(y,0)dy, =-jE\frac{p\cos\varphi}{2\pi}\exp(-j\beta_0 z)\sum_{n=0}^{\infty}P_n(\cos\Delta)\times\left(\frac{1}{n+s}+\frac{1}{n+1-s}\right), =-j\frac{E}{2}\exp(-j\beta_0 z)\frac{p\cos\varphi}{\sin s\pi}P_{-s}(\cos\Delta'). \quad (15)$$

[12] A. Edelyi and others, *Higher Transcendental Functions* (McGraw-Hill Book Company, Inc., 1953), Vol. I, p. 166.

[13] See reference 12, p. 167.

[14] A tabulation of Legendre functions of fractional order $P_{-s}(\cos\theta)$, for $0°<\theta<\pi/2$ only, is available in "Tables des Fonctions de Legendré Associtées," published by Service de Documentation Interministerielle, de Centre National D'Etudes des Telecommunications, Paris (1952). Values of $P_{-s}(\cos\theta)$ for $\pi/2<\theta<\pi$ as needed in the numerical calculations of this paper were computed by Mr. J. Riordan of the Engineering Research Institute, University of Michigan, Ann Arbor, Michigan.

The current flows in the z direction, and the current density on the surface (whose center is at $x=0$) is,

$$J=-jE\left(\frac{\epsilon}{\mu}\right)^{\frac{1}{2}}\exp(-j\beta_0 z)\left(\frac{2}{\cos x-\cos\Delta}\right)^{\frac{1}{2}}\times\exp[-j(s-\tfrac{1}{2})x]\quad(|x|<\Delta).\tag{16}$$

The total current is obtained by integrating J over both sides,

$$I=-j2E\left(\frac{\epsilon}{\mu}\right)^{\frac{1}{2}}\exp(-j\beta_0 z)(p\cos\varphi)P_{-s}(\cos\Delta).\tag{17}$$

The transverse or circuit impedance is therefore,

$$K_t=-\frac{1}{4}\left(\frac{\mu}{\epsilon}\right)^{\frac{1}{2}}\frac{1}{\sin s\pi}\frac{P_{-s}(\cos\Delta')}{P_{-s}(\cos\Delta)}.\tag{18}$$

The current density at the edges of the tapes is infinitely large. Since the square of the current density is *not* integrable over the tape, neither this nor any *tape* model is satisfactory for investigating the *loss* of helical structures. A means for extending the above analysis to wires of finite thickness is seen to be necessary.

SOLUTION FOR WIDE HELICES BY CONFORMAL MAPPING

Solution II_1 may be adapted to other wire configurations by conformal transformation. In Fig. 2(a) and 2(b), for wire cross sections symmetrical with the x' axis, a conformal transformation that maps the cell $A_2B_2C_2D_2E_2F_2G_2$ in x'-y' plane onto $A_1B_1C_1D_1E_1F_1G_1$ in x-y plane provides the correct field behavior for the developed-wire helix. Representing this transformation by:

$$\xi=\xi(\eta),\tag{19}$$

where

$$\xi=x+jy,$$

and

$$\eta=x'+jy',$$

then Eq. (12), expressed in η and its complex conjugate η^*, is the solution for the developed-wire helix, satisfying all the boundary conditions.

Although the power W, voltage V, current I, and hence transverse impedance K_t are invariant through such a transformation, the distribution of fields is changed. To find the actual field configuration, it is necessary to express Eq. (12) in the form,

$$II=-\frac{E}{\beta_0}\frac{p\cos\varphi}{2\pi}\exp(-j\beta_0 z)\times\left\{\sum_{n=0}^{\infty}\frac{b_n}{n+s}\exp[-j(s+n)\eta^*]+\sum_{n=0}^{\infty}\frac{c_n}{n+1-s}\exp[-j(n+1-s)\eta]\right\}.\tag{20}$$

Implicitly from Eq. (19),

$$\exp(-j\xi^*)=a_0\exp(-j\eta^*)\times[1+\sum_{n=1}^{\infty}a_n\exp(-jn\eta^*)],\tag{21}$$

and

$$\exp(j\xi)=a_0^*\exp(j\eta)[1+\sum_{n=1}^{\infty}a_n^*\exp(jn\eta)],\tag{22}$$

where the a_n's are determined by the size and shape of the helix wire. Introducing these equations into Eq. (12) yields,

$$\begin{aligned}
b_0&=P_0(\cos\Delta)a_0^s,\\
b_1&=P_1(\cos\Delta)a_0^{1+s}+P_0(\cos\Delta)(1+s)a_0^s a_1,\\
b_2&=P_2(\cos\Delta)a_0^{2+s}+P_1(\cos\Delta)(2+s)a_0^{1+s}a_1\\
&\quad+P_0(\cos\Delta)(2+s)a_0^s\left[a_2+\frac{s-1}{2}a_1^2\right],\\
c_0&=P_0(\cos\Delta)a_0^{*(1-s)},\\
c_1&=P_1(\cos\Delta)a_0^{*(2-s)}+P_1(\cos\Delta)(2-s)a_0^{*(1-s)}a_1^*,\\
c_2&=P_2(\cos\Delta)a_0^{*(3-s)}+P_1(\cos\Delta)(3-s)a_0^{*(2-s)}a_1^*\\
&\quad+P_0(\cos\Delta)(3-s)a_0^{*(1-s)}\left[a_2^*-\frac{s}{2}a_1^{*2}\right],\quad\text{etc.}
\end{aligned}\tag{23}$$

The coefficients b_0, b_1, b_2, etc., are the relative amplitudes of the fundamental and space-harmonic field components with positive phase velocity (forward waves) along the axis of the developed helix, and c_0, c_1, c_2 are the relative amplitudes of the components with negative phase velocity (backward waves). In tape helices, each harmonic field contributes to the total power independently. However, in thick-wire helices the harmonic fields interact in contributing to the total power. Therefore, the term "harmonic power" is less meaningful when applied to wire helices.

In the transformation of Eq. (19), a scale factor indicating the length of arc in the x'-y' plane transformed from an arc of unit-length in the x-y plane is defined by

$$h(x,y)=|d\eta/d\xi|.\tag{24}$$

Using Eqs. (24) and (16), the current density on the surface of a wire conductor may be expressed as a function of x:

$$J=-j\left(\frac{\epsilon}{\mu}\right)^{\frac{1}{2}}E\exp(-j\beta_0 z)\left(\frac{2}{\cos x-\cos\Delta}\right)^{\frac{1}{2}}\times\frac{\exp[-j(s-\frac{1}{2})x]}{h(x,0)}.\tag{25}$$

Then, the total effective value of $|J|^2$ may be integrated around the surface of the conductor:

$$\sum |J_{\text{eff}}|^2 = \tfrac{1}{2}\int_{\substack{\text{Over the periphery}\\ \text{of a conductor}}} |J|^2 h(x,0)\,dx, \qquad (26)$$

$$= -\frac{2\epsilon}{\pi\mu} E^2 p \cos\varphi L,$$

where

$$L = \int_0^{\Delta} \frac{dx}{h(x,0)(\cos x - \cos\Delta)}. \qquad (27)$$

Thus, if R_0 is the resistance of the wire per unit-linear length per unit-surface width,[15] then the loss per unit-length of the helix wire is,

$$W_L/\text{Length} = R_0 \sum |J_{\text{eff}}|^2. \qquad (28)$$

If the transformation given by Eq. (19) is determinable, the properties of a developed-wire helix can be derived from the tape solution. The pertinent parameters of the transformation are (a) the value of Δ, (b) the values a_0, a_1, a_2, etc., and (c) the function $h(x,0)$.

TRANSFORMATION FOR ELLIPTIC WIRES

Although an exact transformation for circular wire cross sections has been derived by Love[16] in connection with electrostatic problems, his method is too complicated to apply to the present problem. An approximate transformation suggested by Richmond is used to map the nearly elliptical, oval-shaped boundaries into straight lines,[17] since, if the dimension of wire is less than 0.7 of the pitch, the oval shape is within 10 percent of the radius vector of an ellipse. Then Eq. (19) takes the form,

$$\eta = jM \cosh^{-1}\left(\frac{\cos\xi + \sin^2\tfrac{1}{2}\Delta}{\cos^2\tfrac{1}{2}\Delta}\right) + (1-M)\xi, \qquad (29)$$

where the multi-valued function $\cosh^{-1}z$ is restricted by

$$\text{Re}[\cosh^{-1}z] > 0, \qquad (30a)$$

and

$$-\pi < \text{Im}[\cosh^{-1}z] < \pi. \qquad (30b)$$

The values M and Δ are determined from the dimensions of the elliptic wire. If the normalized dimensions are represented by u and v, then:

$$u = (1-M)\Delta, \qquad (31a)$$

and

$$v = 2M \cosh^{-1}(\sec\tfrac{1}{2}\Delta). \qquad (31b)$$

[15] Neglecting the surface conditions, R_0 may be expressed in terms of resistivity ρ, angular frequency ω, and permeability μ: $R_0 = (\rho\omega\mu/2)^{\frac{1}{2}}$.

[16] A. E. H. Love, Quart. J. Math., Oxford Series 9, 246 (1938).

[17] H. W. Richmond, Proc. London Math. Soc. Ser. 2, 22, 389 (1924).

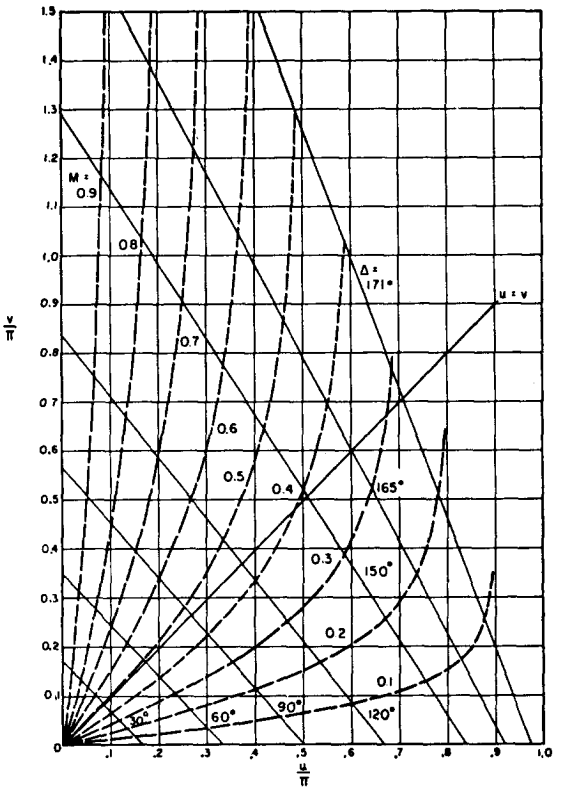

FIG. 3. Curves for reducing an elliptic wire to the equivalent tape.

Solving Eq. (31) for the values of M and Δ produces values for u and v. In Fig. 3, loci of constant M and Δ are plotted in the u-v plane. The straight line $u=v$ in Fig. 3 gives the value of M and Δ for essentially round wires.

From Eq. (29), with some algebraic manipulation, one obtains

$$\frac{d\eta}{d\xi} = (1-M) \pm jM\left(\frac{1-\cos\xi}{\cos\xi - \cos\Delta}\right)^{\frac{1}{2}}. \qquad (32)$$

Therefore,

$$h(x,0) = \left[\frac{M^2 - (1-M)^2\cos\Delta - (2M-1)\cos x}{\cos x - \cos\Delta}\right]^{\frac{1}{2}}. \qquad (33)$$

The coefficients a_0, a_1, etc. can be obtained by expressing Eq. (29) in series form of Eq. (21), yielding:

$$a_0 = \left(\frac{1}{\cos\tfrac{1}{2}\Delta}\right)^{2M},$$

$$a_1 = 2Ma_0 \sin\tfrac{1}{2}\Delta, \qquad (34)$$

$$a_2 = M \sin^2\tfrac{1}{2}\Delta(6M\sin^2\tfrac{1}{2}\Delta - 3\sin^2\tfrac{1}{2}\Delta + 2)a_0^2.$$

Substituting Eq. (33) into Eq. (27) yields the value

of L,

$$L=\int_0^{\Delta}\times\frac{dx}{(\cos x-\cos\Delta)^{\frac{1}{2}}[M^2-(1-M)^2\cos\Delta(2M-1)\cos x]^{\frac{1}{2}}}. \tag{35}$$

This integration can be expressed in terms of complete elliptic integrals of the first kind, $F[(\pi/2), k]$. The result is:

(a) if $$M>\frac{\cos\frac{1}{2}\Delta}{M\sin\frac{1}{2}\Delta},$$

$$L=\left(\frac{1}{M\sin\frac{1}{2}\Delta}\right)F\left(\frac{\pi}{2},k_1\right), \tag{36a}$$

where

$$k_1=\frac{1}{M}[M^2-(1-M)^2\cos^2\tfrac{1}{2}\Delta]^{\frac{1}{2}},$$

and

(b) if $$M<\frac{\cos\frac{1}{2}\Delta}{1+\cos\frac{1}{2}\Delta},$$

$$L=\frac{1}{(1-M)\sin\frac{1}{2}\Delta\cos\frac{1}{2}\Delta}F\left(\frac{\pi}{2},k_2\right) \tag{36b}$$

where

$$k_2=\frac{[(1-M)^2\cos^2\tfrac{1}{2}\Delta-M^2]}{(1-M)\cos\frac{1}{2}\Delta}.$$

With these expressions for L in Eqs. (26) and (28), the attenuation of developed-wire helices can be calculated.

DEVELOPED *VS* TRUE HELIX

The properties and parameters of the true helix differ somewhat from those of the developed model. For example, $(K_t)_{\text{d.w.}}$ for the developed wire (d.w.) model presumably will differ slightly from $(K_t)_{\text{d.w.}}$ for a true, undeveloped wire (t.w.) helix. The extent of such error can be estimated from the comparable error between $(K_t)_{\text{d.s.}}$ and $(K_t)_{\text{t.s.}}$ for a developed sheath (d.s.) and a true sheath (t.s.) helix. Furthermore, assuming that the process of development affects both wire or tape and sheath helices similarly, then the ratios $(K_t)_{\text{d.w.}}/(K_t)_{\text{t.w.}}$ and $(K_t)_{\text{d.s.}}/(K_t)_{\text{t.s.}}$ should be equal, and

$$(K_t)_{\text{t.w.}}=\left(\frac{(K_t)_{\text{d.w.}}}{(K_t)_{\text{d.s.}}}\right)(K_t)_{\text{t.s.}}=R_t(K_t)_{\text{t.s.}}.$$

Thus, if the developed-wire results are normalized in terms of the developed-sheath value, then each property of a wire helix can be obtained by determining the true-sheath value from existing theory, then multiplying this value by the normalizing ratio R.[18]

[18] Reference 1, p. 39.

The solution of a developed sheath helix is simply the first term of Eq. (12). With a subscript (0) to indicate developed sheath values,

$$W_0=\tfrac{1}{2}E^2\left(\frac{\epsilon}{\mu}\right)^{\frac{1}{2}}(p\cos\varphi)^2\frac{1}{s\pi}, \tag{37}$$

$$(K_t)_0=\tfrac{1}{4}\left(\frac{\epsilon}{\mu}\right)^{\frac{1}{2}}\frac{1}{s\pi}, \tag{38}$$

and

$$\sum|J_{\text{eff}}|_0^2=\frac{\epsilon}{\mu}E^2p\cos\varphi. \tag{39}$$

Comparing these equations with the corresponding values for the developed-wire helix yields

(a) characteristic impedance

$$K_t=(K_t)_0R_t, \tag{40}$$

where

$$R_t=\frac{s\pi}{\sin s\pi}\frac{P_{-s}(\cos\Delta')}{P_{-s}(\cos\Delta)}; \tag{41}$$

(b) attenuation

$$\alpha=(\alpha)_0R_\alpha, \tag{42}$$

where

$$R_\alpha=\frac{2}{\pi}\frac{L}{\frac{s\pi}{\sin s\pi}P_{-s}(\cos\Delta)P_{-s}(\cos\Delta')}; \tag{43}$$

(c) beam-coupling impedance

$$K=\frac{E^2}{2\beta^2W}=K_0R_k, \tag{44}$$

where, for zeroth mode operation and if the interaction field E is taken at the center of the helix,

$$R_{k(c)}=\left(\frac{1}{\cos^2\frac{1}{2}\Delta}\right)^{2sM}\frac{1}{\frac{s\pi}{\sin s\pi}P_{-s}(\cos\Delta)P_{-s}(\cos\Delta')}, \tag{45}$$

or, if the maximum available field at the edge of the conductors is used,

$$R_{k(e)}=\left(\frac{1}{\cos^2\frac{1}{2}\Delta}\right)^{2sM}\frac{\exp(-2sv)}{\frac{s\pi}{\sin s\pi}P_{-s}(\cos\Delta)P_{-s}(\cos\Delta')}. \tag{46}$$

For any other mode of operation, it is evident from Eqs. (20) and (22) that $R_{k(c)}$ should be multiplied by the factor $|b_ns/b_0(n+s)|^2$ for any forward wave, and by $|c_ns/b_0(n-1+s)|^2$ for any backward wave opera-

tion.[19] Similar multipliers for $R_{k(\phi)}$ can be obtained easily.

The normalizing ratios so obtained are functions of three variables: s, Δ, and M. The variables M and Δ are wire size and shape parameters. The variable s is essentially the frequency parameter. In the developed model, s is linearly proportional to frequency (devoid of phase dispersion). For a true helix, a reasonable value of s should be calculated from the value of β for the sheath helix of the same pitch and pitch angle.

MULTIFILAR HELICES

The generating section of a developed *uniform*, m-filar helix can be considered as a cascade of m identical sections of some monofilar helix; so the parameters can be directly evaluated by monofilar analysis. As shown in Fig. 4, the one-to-one correspondence of the dimensions of an m-filar developed helix with that of its generating monofilar section leads to the following relations:

[m-filar developed helix]		[m-filar generating section]
Pitch angle	φ	φ
Pitch	p	p/m
Normalized wire size	u,v	mu,mv
Constants for transformation to equivalent tape	M,Δ	M_m,Δ_m
Frequency parameter	s	s_m

where M,Δ are obtained from Eq. (31) using u and v, M_m,Δ_m are similarly obtained for mu and mv, and s_m is obtained from

$$[e^{-js}m]^m=e^{-js}, \tag{47}$$

or

$$s_m=\frac{s}{m},\ \frac{s+1}{m},\ \frac{s+2}{m},\ \cdots\frac{s+m-1}{m}. \tag{48}$$

In other words, in an m-filar helix there are m-independent modes corresponding to the m values of s_m. Using the values of s_m and the reduced pitch in Eq. (12) one obtains the well-known properties of a multifilar helix:

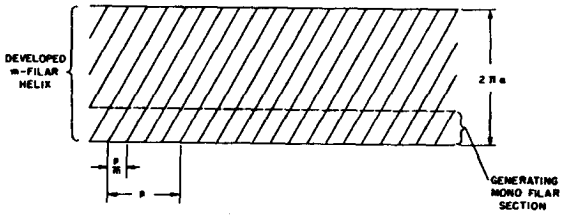

FIG. 4. Developed m-filar helix and its generating monofilar section.

[19] In particular, the backward wave corresponding to c_0 is most widely used. See D. A. Watkins and E. A. Ash, J. Appl. Phys. 25, 782 (1954).

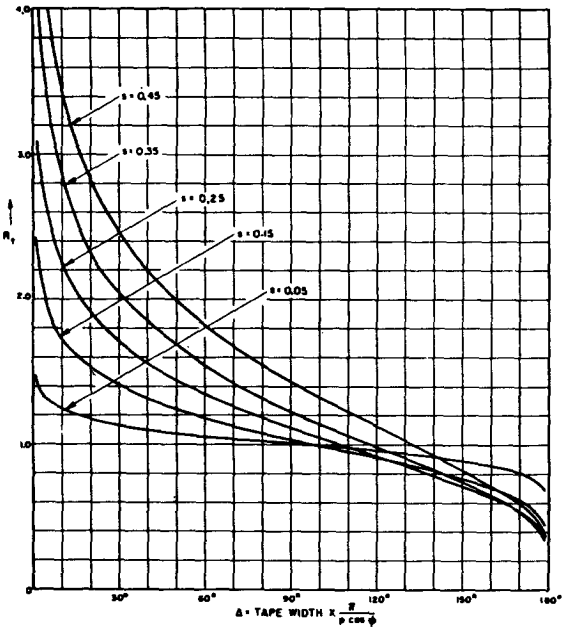

FIG. 5. Variation of transverse impedance with tape width.

(a) the space harmonics are spread m-time apart as compared to a single-filar helix, and
(b) only the symmetric mode, $s_m=s/m$, produces the fundamental field of a single-filar helix.

For the symmetric mode, the power propagated along a developed m-filar helix is:

$$W_m=\frac{1}{2m}\left(\frac{\epsilon}{\mu}\right)^{\frac{1}{2}}E_0^2(p\cos\varphi)^2\frac{1}{\sin\frac{s\pi}{m}}\times P_{-s/m}(\cos\Delta_m)P_{-s/m}(\cos\Delta_m'), \tag{49}$$

and the loss per unit-length of the helix wire:

$$(W_L/\text{length})_m=R_0\frac{2}{\pi}\frac{\epsilon}{\mu}\frac{1}{m}E^2(p\cos\varphi)L(M_m,\Delta_m). \tag{50}$$

Therefore, the following relation is obtained:

$$\frac{(\alpha)_{m\text{-filar}}}{(\alpha)_{\text{single-filar}}}=\frac{R_\alpha\left(M_m,\Delta_m,\frac{s}{m}\right)}{R_\alpha(M,\Delta,s)}. \tag{51}$$

Similarly, for the coupling impedance:

$$\frac{(K)_{m\text{-filar}}}{(K)_{\text{single-filar}}}=\frac{R_k\left(M_m,\Delta_m,\frac{s}{m}\right)}{R_k(M,\Delta,s)}. \tag{52}$$

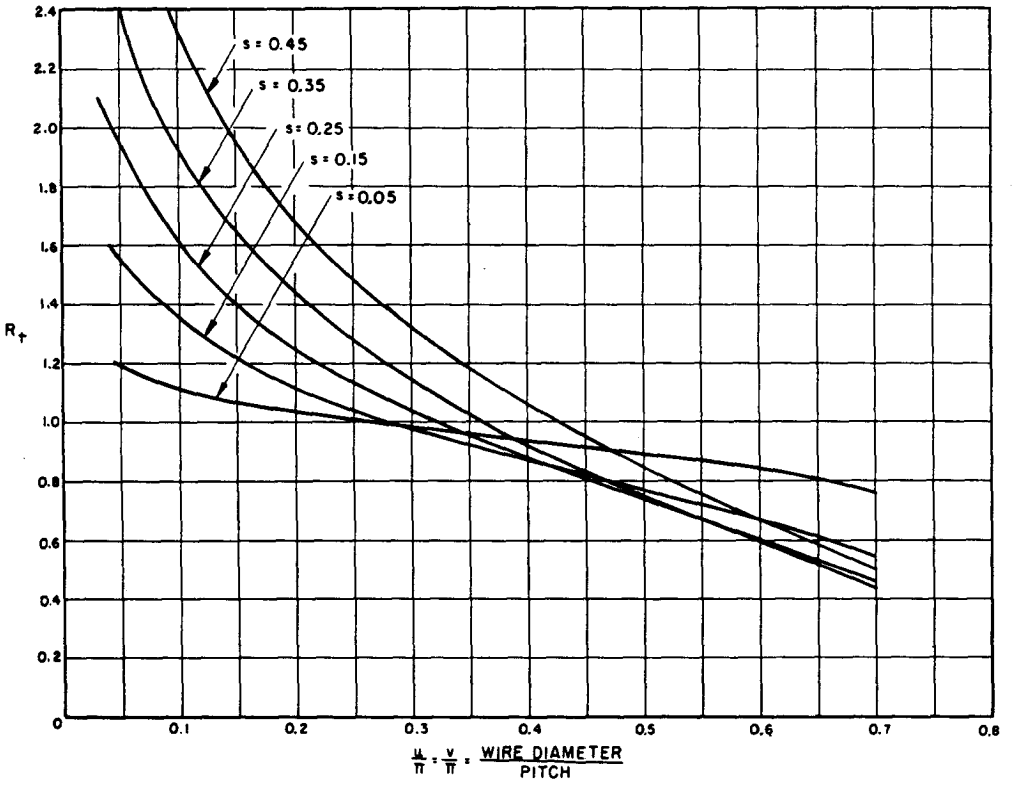

FIG. 6. Effect of wire diameter on the transverse impedance of a helix.

One can generalize Eqs. (52) and (53) and obtain the ratio of the value of attenuation or coupling impedance of an m-filar helix of normalized conductor size v,u to the corresponding value of an n filar one of normalized size v', u'. The ratios resulting are:

$$\frac{\alpha_{m\text{-filar }(u,v)}}{\alpha_{n\text{-filar }(u',v')}} = \frac{R_\alpha\left[mu, mv, \frac{s}{m}\right]}{R_\alpha\left[nu', nv', \frac{s}{n}\right]} \tag{53}$$

and

$$\frac{K_{m\text{-filar }(u,v)}}{K_{n\text{-filar }(u',v')}} = \frac{R_k\left[mu, mv, \frac{s}{m}\right]}{R_k\left[nu', nv', \frac{s}{n}\right]}. \tag{54}$$

Graphical data illustrating the above comparisons are presented in the following section.

NUMERICAL RESULTS

The effects of wire size and shape on the helix parameters are presented in graphs of the various correction factors R_α, R_k, and R_t as functions of the several parameters connected with wire size for several selected values of the phase parameter s.

In Fig. 5, the transverse-impedance factor R_t is plotted *vs* the transformed-wire parameter Δ. This factor is independent of M. (Values Δ and M corresponding to specified u and v are given in Fig. 3.) For round wires R_t is replotted *vs* wire-diameter-to-helix-pitch ratio u/π in Fig. 6. These curves agree very well with the analysis given by Pierce[20] for $s=0.25$ for a wide range of diameter-to-pitch ratio.

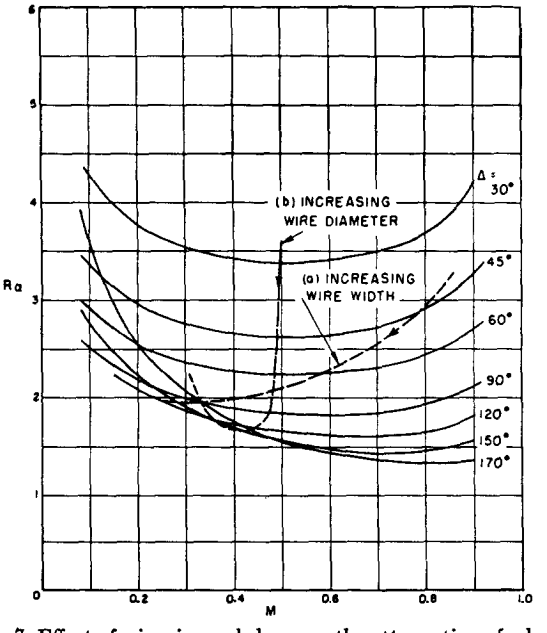

FIG. 7. Effect of wire size and shape on the attenuation of a helix. ($s=0.4$) (a) Elliptic wire of fixed thickness (b) circular wire.

[20] See reference 1, p. 40.

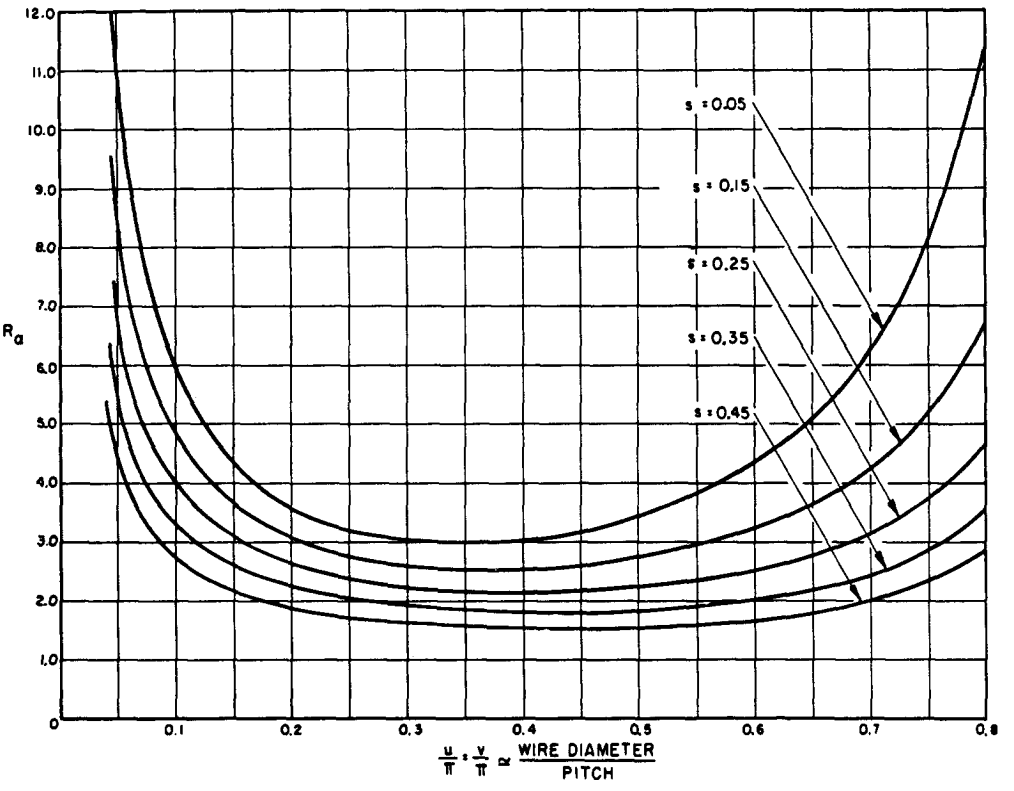

FIG. 8. Effect of wire diameter on the attenuation of a helix.

The typical variation of the attenuation factor R_α *vs* the wire parameters Δ and M is shown in Fig. 7 ($s=0.4$). The locus of R_α for wires of constant radial thickness but with varying width is shown as a superimposed curve (a). For a fixed thickness of wire, there is a critical width that gives least attenuation. Similarly, the locus of R_α for round wires *vs* M is shown in curve (b). This indicates a critical diameter-to-pitch ratio for least attenuation. In Fig. 8 the variation of R_α *vs* u/π for circular wires is shown for several values of s. These results, as far as variation of attenuation with wire size is concerned, agree remarkably well with the experimental results given by Peter.[21] The exact value of attenuation was not calculated, because the exact resistivity of the wire used is not known.

One is tempted to use the above curves to determine an optimized wire cross section for minimum attenuation. But direct use of the curves is not meaningful; for, as indicated by Fig. 7, R_α is minimized if $M\rightarrow 1.0$ and $\Delta\rightarrow 180°$; that is, on use of a thin tape of infinite width in the radial direction. This physically impossible result is a consequence of the use of the developed model as opposed to a true-helix model. In a true helix, as the radial thickness becomes comparable to the mean-helix radius, the proximity of current between opposite sides of a turn of the helix would introduce more and more unaccounted-for coupling, and thus nullify the validity of deductions from the developed model.

[21] Peter, Ruetz, and Olson, R.C.A. Rev. 13, 558 (1952).

Similar curves for the coupling impedance R_k are presented in Fig. 9 and Fig. 10. In Fig. 9, R_k is evaluated with reference to the field at the center of the helix; in Fig. 10, with reference to the field at the edge of the wire (maximum available field). With reference to the field at the center of the helix, optimizing of the

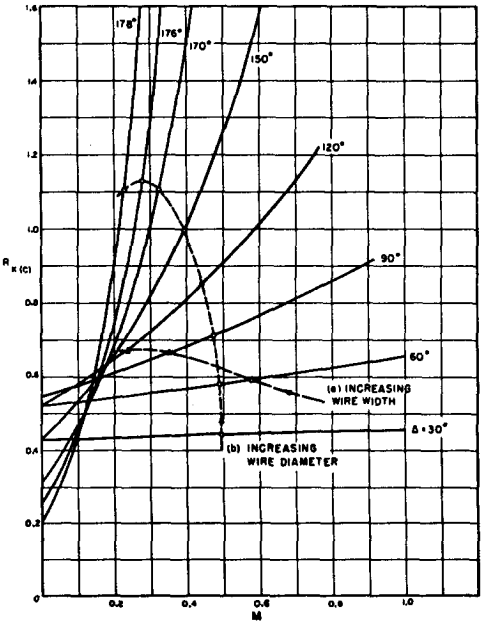

FIG. 9. Effect of wire size and shape on the coupling impedance of a helix. Comparison based on field at center of helix. ($s=0.4$) (a) Elliptic wire of fixed thickness (b) circular wire.

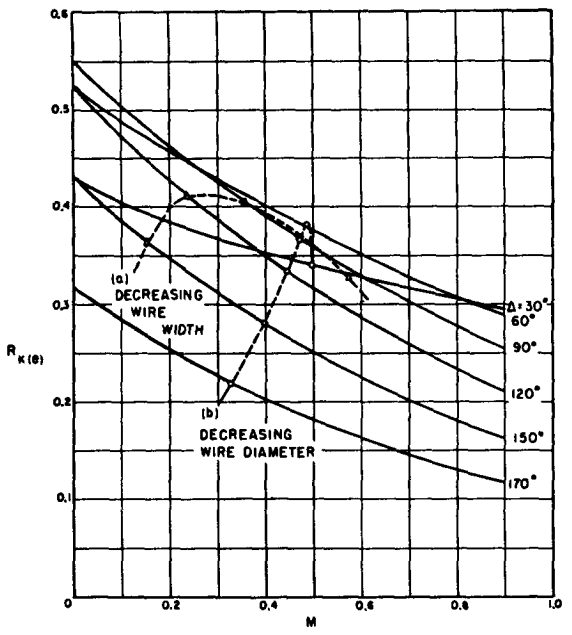

FIG. 10. Effect of wire size and shape on the coupling impedance of a helix. Comparison based on the field at the edge of the wire ($s=0.4$). (a) Elliptic wire of fixed thickness (b) circular wire.

wire configuration for highest K leads to the same impossible result as that for optimizing R_α. However, with reference to the maximum-available field, R_k is highest for thin tapes occupying half the pitch width, as indicated by Fig. 10.

For round wires, the effect of wire size on the coupling-impedance factor R_k is shown by Fig. 11 and Fig. 12. The curves for $s=0.25$, corresponding to approximately four turns per wavelength, agree well with the result given by Pierce[22] in the range of wire size at which the transformation is accurate. Again critical sizes of wire are indicated for maximum R_k.

A comparison between the parameters of any specified multifilar helix and those of a monofilar one can be obtained from Eqs. (53) and (54).

Two particular cases of interest are: (a) comparison of helices utilizing identically-shaped conductors and identical conductor-width-to-gap-width ratios, and (b) alternatively, comparison of helices utilizing identically-shaped conductors and identical conductor widths. In the former case, the width/pitch ratio of the equivalent generating section of the multifilar helix is the same as that of the monofilar reference of the same pitch. Any change of R_α and R_k hence is due only to the change of the phase parameters from s in the reference to s_m in the generating section.

Therefore one can see from Figs. 8, 11, and 12, that, for circular wires of specified dia/gap ratio, the attenuation, and the coupling impedance based on the field at the edge of wire, always *increase* as the number of files of the helix is increased; the coupling impedance based on the field at the center of helix will increase as the number of files is increased *only if* the dia/gap ratio is less than unity.

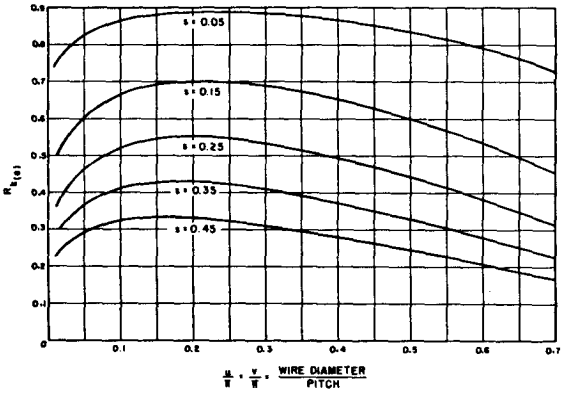

FIG. 12. Effect of wire diameter on the coupling impedance of a helix. (Comparison based on the field at the edge of the wire.)

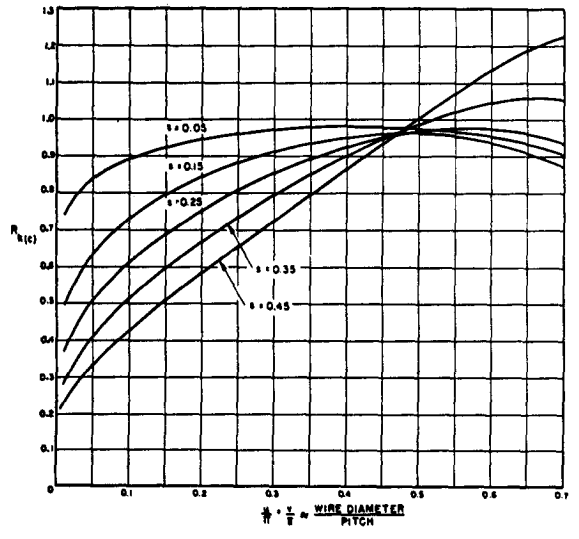

FIG. 11. Effect of wire diameter on the coupling impedance of a helix. (Comparison based on the field at center.)

For the second case mentioned, the results of comparison are more involved, and are shown in Figs. 13 and 14. In Fig. 13, the ratio of attenuation of an m-filar helix to that of a monofilar helix of the same wire size is plotted as a function of wire dia/pitch ratio. In Fig. 14, the ratio of coupling impedance K (same for K_c and K_e) is similarly plotted. One may see from these figures that the attenuation of a multifilar helix is not lower, and the coupling impedance is not higher, than the corresponding values for a monofilar helix except for very small wire diameters.

This comparison between a multifilar and a monofilar helix is based on the assumption that only the symmetric mode of propagation is excited in the multifilar helix. Partial excitation of asymmetric modes would invariably increase the attenuation and decrease the coupling impedances.

[22] See reference 1, p. 39.

CONCLUSIONS

This analysis makes possible the calculation of the parameters of wire helices with reasonable accuracy. In particular, it provides a sound basis for calculating the attenuation, for which no adequate theoretical analysis has been available previously.

Inaccuracies introduced into the analysis in approximating the true helix with a developed model are partially compensated by expressing all results as the product of a proper correction factor times the corresponding known value for a sheath helix. The residual inaccuracy should be slight as long as the thickness and width of the conductor are negligible in comparison with the diameter of helix.

The effect of wire size and shape on the attenuation

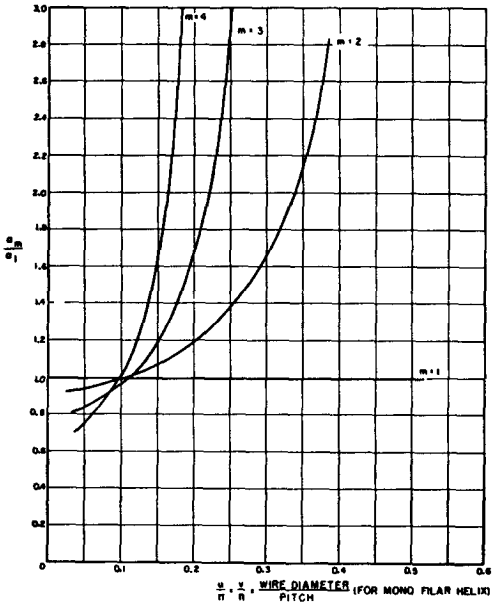

FIG. 13. Ratio of the attenuation of a m-filar helix to that of a single filar helix with same wire diameter and pitch angle ($s=0.45$).

and other helix propagation parameters for both monofilar and multifilar helices has been clarified and quantitatively calculated.

It is shown that for round wires there are critical values of dia/pitch ratio for minimum attenuation and for highest coupling impedance. The calculated attenuation characteristics agree well with experimental data obtained by others.

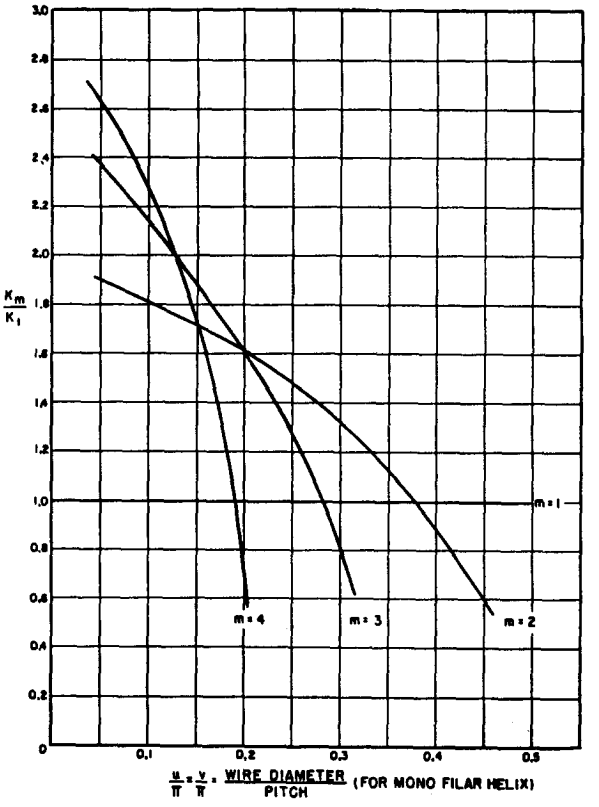

FIG. 14. Ratio of coupling impedance of a m-filar helix to that of a monofilar helix with same wire diameter and pitch angle ($s=0.45$).

It is also seen that multifilar helices of circular wires have little or no advantage over monofilar ones so far as attenuation is concerned.

ACKNOWLEDGMENTS

The author wishes to express his appreciation to W. E. Vivian of the Engineering Research Institute, The University of Michigan, for his constructive criticism during the progress of this work, and to Professor G. Hok and Mr. M. H. Miller of the Electrical Engineering Department, The University of Michigan, for their aid in editing the manuscript. The author is grateful to Mr. J. Riordan of the Engineering Research Institute, The University of Michigan, for his labors in carrying out the computations.